

Supplementary Information

Label-free and near-zero-background-noise photoelectrochemical assay of methyltransferase activity based on Bi₂S₃/Ti₃C₂ Schottky junction

Yamin Fu^a, Feng Ding^a, Jinhua Chen^{a,*}, Mengyue Liu^a, Xiaohua Zhang^a, Cuicui Du^a, and Shihui Si^{b,*}

^aState Key Laboratory of Chemo/Biosensing and Chemometrics, College of Chemistry and Chemical Engineering, Hunan University, Changsha, 410082, P.R. China

^bCollege of Chemistry and Chemical Engineering, Central South University, Changsha 410083, P.R. China

List of Contents:

- 1. Materials and reagents**
- 2. Apparatus**
- 3. Preparation of Ti₃C₂ MXene**
- 4. Synthesis of Bi₂S₃/Ti₃C₂ nanosheets**
- 5. Construction of the PEC sensing platform and PEC assay of M.SssI Mtase**
- 6. XRD patterns of Ti₃C₂ MXene and Ti₃AlC₂**
- 7. FTIR spectrum of Ti₃C₂ MXene.**
- 8. EIS characterization of Ti₃C₂/GC electrode**

* Corresponding author. Tel.: +86-731-88821848
E-mail address: chenjinhua@hnu.edu.cn; sishihui@163.com

- 9. HRTEM image of $\text{Bi}_2\text{S}_3/\text{Ti}_3\text{C}_2$ nanosheets**
- 10. EDS spectrum of $\text{Bi}_2\text{S}_3/\text{Ti}_3\text{C}_2$ nanosheets.**
- 11. XRD pattern of $\text{Bi}_2\text{S}_3/\text{Ti}_3\text{C}_2$ nanosheets**
- 12. XPS spectrum of $\text{Bi}_2\text{S}_3/\text{Ti}_3\text{C}_2$ nanosheets**
- 13. Cathodic and anodic linear potential scans of Bi_2S_3**
- 14. The feasibility of the developed PEC biosensing platform**
- 15. Optimization of experimental conditions**
- 16. Comparison of various PEC biosensors for M.SssI MTase activity assay**
- 17. Selectivity, stability, reproducibility and recovery test**
- 18. Efficiency of different inhibitors on M.SssI MTase activity**
- 19. References**

1. Materials and reagents

Ti₃AlC₂ and 3-aminopropyltriethoxysilane (APTES) were obtained from Shanghai Maclean Biochemical Technology Co., Ltd. (Shanghai, China). Procaine, LiF and 5-aza-2'-deoxycytidine (5-Aza-dC) were purchased from Aladdin Chemistry Co., Ltd. (Shanghai, China). Bi(NO₃)₃·5H₂O, Na₂S·9H₂O, L-Cysteine (L-Cys) and glutaraldehyde (GA) were supplied by Sinopharm Chemical Reagent Co., Ltd. (Beijing, China). S-adenosylmethionine (SAM), M.SssI CpG methyltransferase (M.SssI MTase) supplied with 10 × NEBuffer 2, Dam methyltransferase (Dam MTase), AluI methyltransferase (AluI MTase) and restriction endonuclease HpaII supplied with 10 × CutSmart buffer were acquired from New England Biolabs (Beijing, China) LTD. The oligonucleotides (S1, 5' - NH₂ - (CH₂)₆- CAG TCC GGA GGT GAA CCT TAG ATA GAC CAA TTA - 3'; S2, 5'-CAC CTC CGG ACT G - 3') and bovine serum albumin (BSA) were obtained from Shanghai Sangon Biotech Co., Ltd. (Shanghai, China). The ITO slides were provided by Zhuhai Kaivo Electronic Components Co., Ltd. (Zhuhai, China). Ultrapure water (18.2 MΩ·cm) used in this work was obtained from Milli-Q water purification system (Millipore Corp., Bedford, MA).

2. Apparatus

The transmission electron microscope (TEM) images were conducted on JEM-2100F (Joel, Japan). Fourier transform infrared (FT-IR) spectrum was measured on FT-IR spectrometric spectrophotometer (Nicolet 6700, USA). Powder X-ray diffraction (XRD)

tests were carried out on X-ray diffractometer (XRD-6100, Japan). UV-visible (UV-vis) spectra were recorded on a UV-2100 spectrophotometer (Beijing Lab Tech, China). X-ray photoelectron spectroscopy (XPS) measurements were carried out on an ESCALAB 250 Xi spectrometer (Thermo Fisher-VG Scientific). PEC and electrochemical impedance spectroscopy (EIS) experiments were performed on an electrochemical workstation (CHI 660B, China) with a three-electrode system including a platinum wire as auxiliary electrode, a modified ITO electrode (diameter, 5.6 mm) as working electrode and a saturated calomel electrode (SCE) as reference electrode. PEC tests were conducted with a 300 W Xe lamp fitted with a 420 nm UV filter (Perfect Light, Beijing) as irradiation source.

3. Preparation of Ti_3C_2 MXene

The delaminated Ti_3C_2 MXene was prepared according to the reported literatures with a little modification.^[1] Typically, LiF (1.5 g) was slowly added in HCl solution (9 M, 20 mL) and the mixture was stirred until LiF was dissolved entirely. Then, Ti_3AlC_2 powder (1 g) was added into the above solution under stirring for 24 h at 35 °C. Subsequently, the mixture was centrifuged and washed by ultrapure water until the pH was 6. The obtained product was re-dispersed in ultrapure water (100 mL) under sonication for 1 h. After that, the dispersion was shaken for 0.5 h and centrifuged at a low speed. Finally, the supernatant was collected, centrifuged and the sediment was re-dissolved into ultrapure water (100 mL) to obtain the delaminated Ti_3C_2 MXene solution.

4. Synthesis of Bi₂S₃/Ti₃C₂ nanosheets

Firstly, 10 mL of the above Ti₃C₂ MXene solution was diluted to 50 mL by ultrapure water. Then, 100 mg of L-cystein (L-Cys) was added into the diluted Ti₃C₂ MXene solution under stirring. On the other hand, 24.3 mg of Bi(NO₃)₃·5H₂O and 24.0 mg of Na₂S·9H₂O were dissolved in 5 mL ultrapure water, respectively. After that, Bi(NO₃)₃ solution was dropped into the above Ti₃C₂ MXene mixture solution slowly, followed by addition of Na₂S solution. After stirred overnight, the mixture was centrifuged and washed by ultrapure water for three times. The collected black precipitation (Bi₂S₃/Ti₃C₂ nanosheets) was re-dispersed in 50 mL ultrapure water and the solution (the concentration of Bi₂S₃/Ti₃C₂ nanosheets, about 2.5 mg mL⁻¹) was kept at 4 °C for the further use.

For comparison, Bi₂S₃ was prepared under the similar procedure without Ti₃C₂ MXene and L-Cys.

5. Construction of the PEC sensing platform and PEC assay of M.SssI MTase

Before use, the ITO electrode was cleaned according to the procedure reported in the previous work.^[2] Then, the ITO electrode was immersed into 2 wt.% APTES overnight, followed by washing with ethanol and dried at 60 °C to obtain the amino-functionalized ITO electrode. Subsequently, GA solution (20 μL, 2.5 wt.%), as a crosslinking agent, was dropped onto the amino-functionalized ITO electrode for 2 h. On the other hand, 10 μL of DNA s1 (2 μM) and 10 μL of DNA s2 (2 μM) were denatured at 95 °C for 5 min,

followed by cooling down to room temperature (25 °C) to obtain dsDNA. Then, 20 μL of dsDNA was placed onto the above ITO electrode for 2 h to obtain the dsDNA/ITO electrode. To restrain the nonspecific adsorption, the prepared dsDNA/ITO electrode was incubated with BSA solution (1 wt.%, 20 μL) for 1 h. After that, the BSA/dsDNA/ITO electrode was incubated with M.SssI MTase solution (different concentrations, 20 μL) containing SAM (160 μM) for 2 h at 37 °C to obtain methylated DNA. Next, 20 μL of HpaII was dropped onto the electrode at 37 °C for 2h to cleave unmethylated DNA. Finally, the electrode was immersed into the $\text{Bi}_2\text{S}_3/\text{Ti}_3\text{C}_2$ nanosheets suspension for 80 min. After washing with Tris-HCl buffer (pH 7.4), the PEC assay was performed in 10 mM Tris-HCl buffer (pH 7.4) at 0 V.

6. XRD patterns of Ti_3C_2 MXene and Ti_3AlC_2

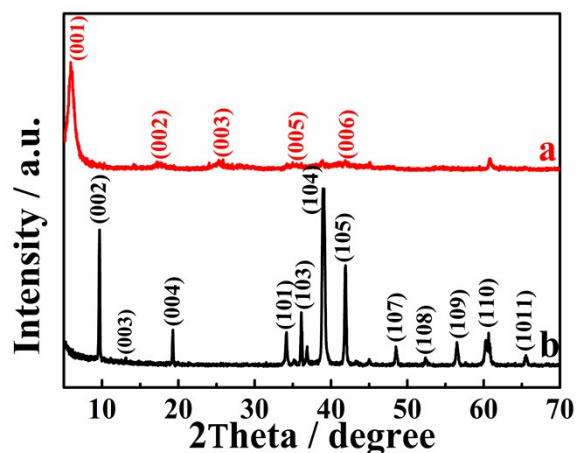


Fig. S1 XRD patterns of Ti_3C_2 MXene (a) and Ti_3AlC_2 (b).

7. FTIR spectrum of Ti_3C_2 MXene.

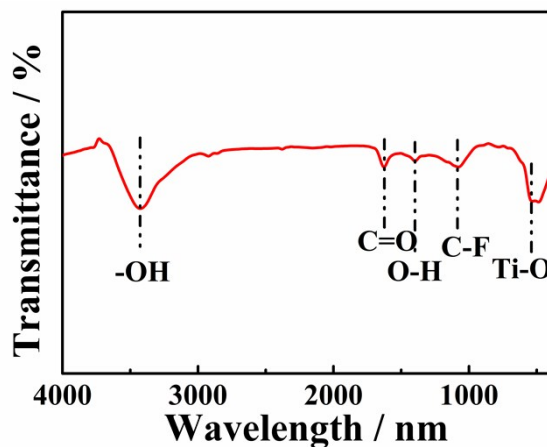


Fig. S2 FTIR spectrum of Ti_3C_2 MXene.

8. EIS characterization of $\text{Ti}_3\text{C}_2/\text{GC}$ electrode

Electrochemical impedance spectroscopy (EIS) was used to estimate the charge transfer property of Ti_3C_2 MXene (Fig. S3). In the electrochemical impedance spectrum, the semicircle section represents the charge-transfer limited process and its diameter is related to the interfacial charge-transfer resistance (R_{ct}). It is noted that the $\text{Ti}_3\text{C}_2/\text{GC}$ electrode has a small domain and the related R_{ct} value (curve b, $R_{\text{ct}} = 0.02 \Omega$) is much smaller than that of the bare glassy carbon electrode (curve a, $R_{\text{ct}} = 212.8 \Omega$), showing an excellent charge-transfer ability.

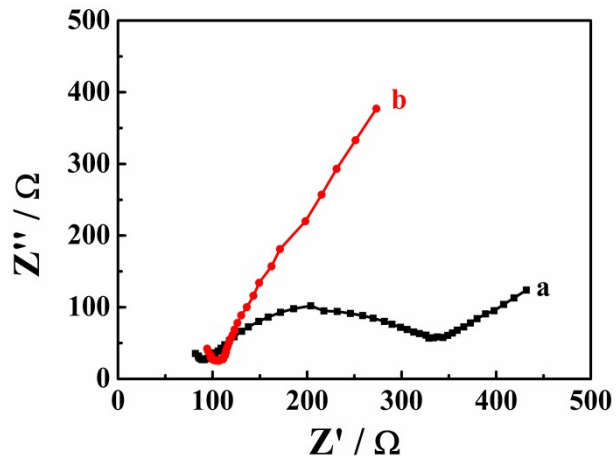


Fig. S3 Nyquist plots of glassy carbon (GC) electrode (curve a) and $\text{Ti}_3\text{C}_2/\text{GC}$ electrode (curve b) in 5 mM $[\text{Fe}(\text{CN})_6]^{3-/4-}$ containing 0.1 M KCl (Potential: open circuit potential; Amplitude, 5 mV; Frequency range, 0.1-100 kHz).

9. HRTEM image of $\text{Bi}_2\text{S}_3/\text{Ti}_3\text{C}_2$ nanosheets

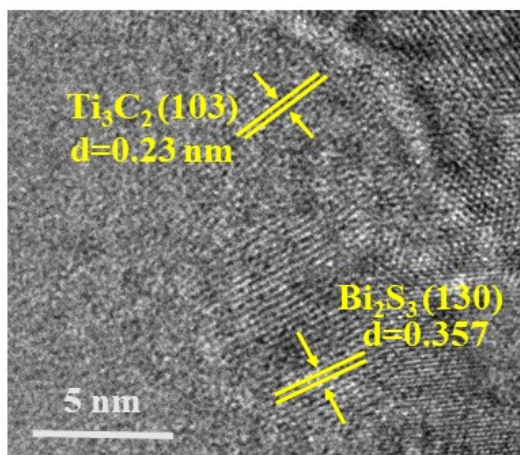


Fig. S4 HRTEM image of $\text{Bi}_2\text{S}_3/\text{Ti}_3\text{C}_2$ nanosheets.

10. EDS spectrum of $\text{Bi}_2\text{S}_3/\text{Ti}_3\text{C}_2$ nanosheets.

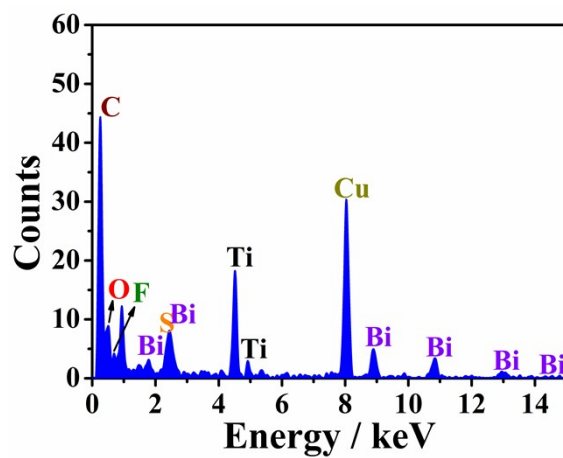


Fig. S5 EDS spectrum of $\text{Bi}_2\text{S}_3/\text{Ti}_3\text{C}_2$ nanosheets.

11. XRD pattern of $\text{Bi}_2\text{S}_3/\text{Ti}_3\text{C}_2$ nanosheets

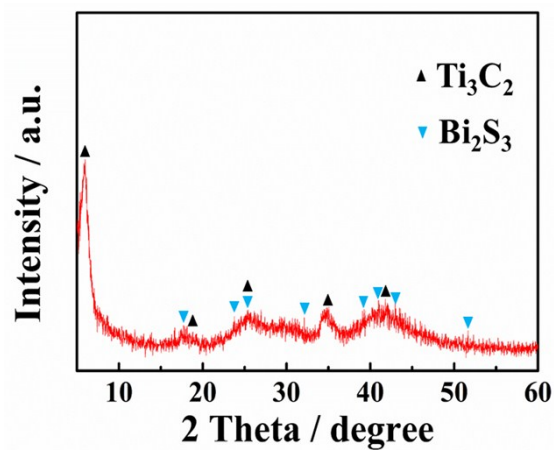


Fig. S6 XRD pattern of $\text{Bi}_2\text{S}_3/\text{Ti}_3\text{C}_2$ nanosheets.

12. XPS spectrum of $\text{Bi}_2\text{S}_3/\text{Ti}_3\text{C}_2$ nanosheets

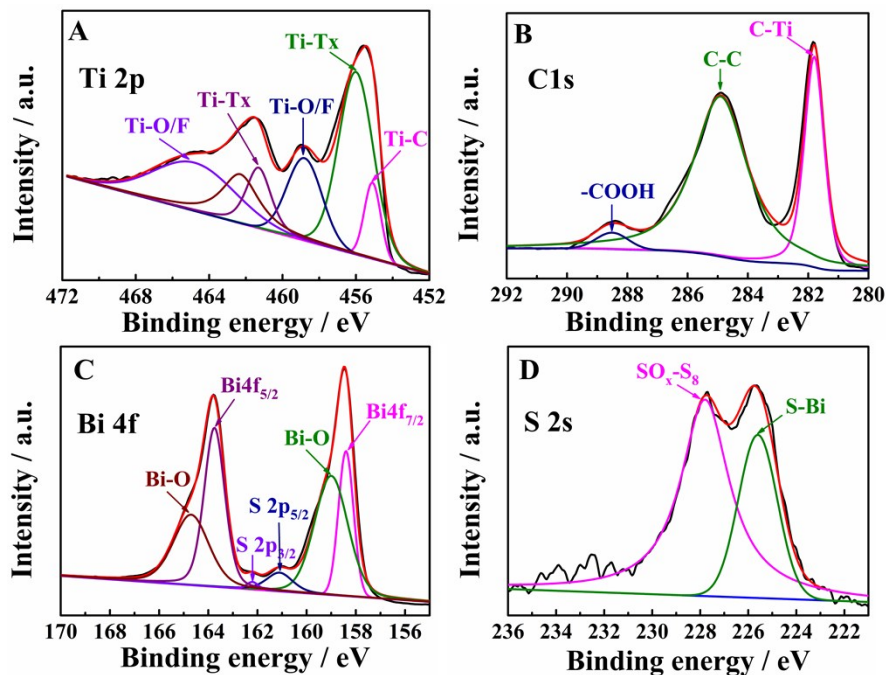


Fig. S7 High-resolution XPS spectra of Ti 2p (A), C 1s (B), Bi 4f (C) and S 2s (D) of $\text{Bi}_2\text{S}_3/\text{Ti}_3\text{C}_2$ nanosheets.

13. Cathodic and anodic linear potential scans of Bi_2S_3

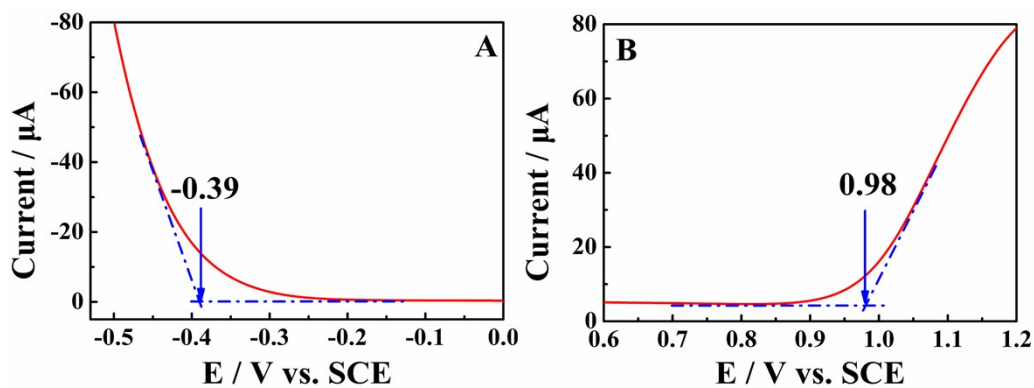


Fig. S8 Cathodic and anodic linear potential scans for determining the conduction band (CB) and valence band (VB) edges of Bi_2S_3 in N_2 -saturated Tris-HCl solution (10 mM,

pH 7.4).

14. The feasibility of the developed PEC biosensing platform

In order to show the feasibility of the developed PEC biosensing platform in M.SssI MTase activity assay, a comparison study was carried out and the corresponding results are presented in Fig. S9. When the concentration of M.SssI MTase is 0, the dsDNA on the BSA/dsDNA/ITO electrode can not be methylated and cleaved completely by HpaII. The residual dsDNA can not obviously adsorb $\text{Bi}_2\text{S}_3/\text{Ti}_3\text{C}_2$ nanosheets due to the weak interaction between dsDNA and Ti_3C_2 nanosheets^[3], resulting in a near-zero photocurrent (in other word, a near-zero background photocurrent) (Fig. S9A). However, when the BSA/dsDNA/ITO electrode is treated with M.SssI MTase (30 U mL^{-1}) and HpaII (50 U mL^{-1}), parts of dsDNA are methylated and can not be cleaved by HpaII. When the electrode is further incubated with $\text{Bi}_2\text{S}_3/\text{Ti}_3\text{C}_2$ nanosheets, the $\text{Bi}_2\text{S}_3/\text{Ti}_3\text{C}_2$ nanosheets are adsorbed on the ssDNA part of the dsDNA, resulting in an obvious photocurrent ($15 \mu\text{A}$) (Fig. S9B). These results indicate clearly that the proposed PEC biosensing platform can be used in M.SssI MTase activity assay with a near-zero-background noise.

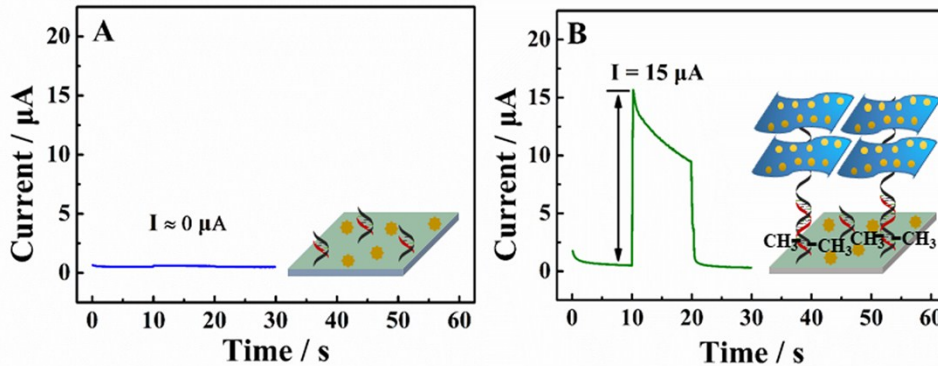


Fig. S9 Photocurrent responses of the BSA/dsDNA/ITO electrode treated with 0 (A) or 30 U mL⁻¹ (B) M.SssI MTase, 50 U mL⁻¹ HpaII, and then incubated with Bi₂S₃/Ti₃C₂ nanosheets for 80 min. The PEC experiments were carried out in 10 mM Tris-HCl (pH 7.4) at 0 V.

15. Optimization of experimental conditions

To achieve the optimal performance of the proposed biosensing platform for M.SssI MTase assay, the mass ratio between Bi₂S₃ and Ti₃C₂, the concentration of Bi₂S₃/Ti₃C₂, the incubation time of M.SssI MTase and the adsorption time of Bi₂S₃/Ti₃C₂ were optimized.

From Fig. S10A, the photocurrent increases with the increase of the mass ratio of Bi₂S₃/Ti₃C₂ and a maximum is observed at 0.5. When the mass ratio of Bi₂S₃/Ti₃C₂ is more than 0.5, the photocurrent decreases. The possible reason is as follows: Under visible light illumination, Bi₂S₃ generates electrons/holes and Ti₃C₂ serves as electron sink due to its near zero bandgap.^[4] When the amount of Bi₂S₃ increases, more electrons/holes pairs are generated, resulting in the increase of the photocurrent. However,

when the mass ratio of $\text{Bi}_2\text{S}_3/\text{Ti}_3\text{C}_2$ is more than 0.5, the high mass ratio of $\text{Bi}_2\text{S}_3/\text{Ti}_3\text{C}_2$ may weaken the interaction between Ti_3C_2 nanosheets and ssDNA, resulting in that the less $\text{Bi}_2\text{S}_3/\text{Ti}_3\text{C}_2$ nanosheets are adsorbed on the ssDNA. Therefore, the photocurrent decreases. Thus, 0.5 is selected as the optimal mass ratio of $\text{Bi}_2\text{S}_3/\text{Ti}_3\text{C}_2$.

The concentration of $\text{Bi}_2\text{S}_3/\text{Ti}_3\text{C}_2$ is another key factor for the proposed biosensor. From Fig. S10B, it is clear that the photocurrent increases with the increase of $\text{Bi}_2\text{S}_3/\text{Ti}_3\text{C}_2$ concentration and then reaches a plateau at 2.5 mg mL^{-1} . So, the optimal concentration of $\text{Bi}_2\text{S}_3/\text{Ti}_3\text{C}_2$ is 2.5 mg mL^{-1} .

The incubation time of M.SssI MTase was also be optimized. From Fig. S10C, it is noted that the photocurrent increases with the increase of incubation time and a plateau reaches at 2.0 h. Therefore, 2.0 h is selected as the optimized incubation time of M.SssI MTase.

In addition, the photocurrent of the developed biosensor increases with the increase of the adsorption time of $\text{Bi}_2\text{S}_3/\text{Ti}_3\text{C}_2$ nanosheets and gradually reaches to a plateau (Fig. S10D), indicating that the amount of adsorbed $\text{Bi}_2\text{S}_3/\text{Ti}_3\text{C}_2$ nanosheets gradually reaches to a saturation. Thus, 80 min is selected as the optimized adsorption time of $\text{Bi}_2\text{S}_3/\text{Ti}_3\text{C}_2$ nanosheets.

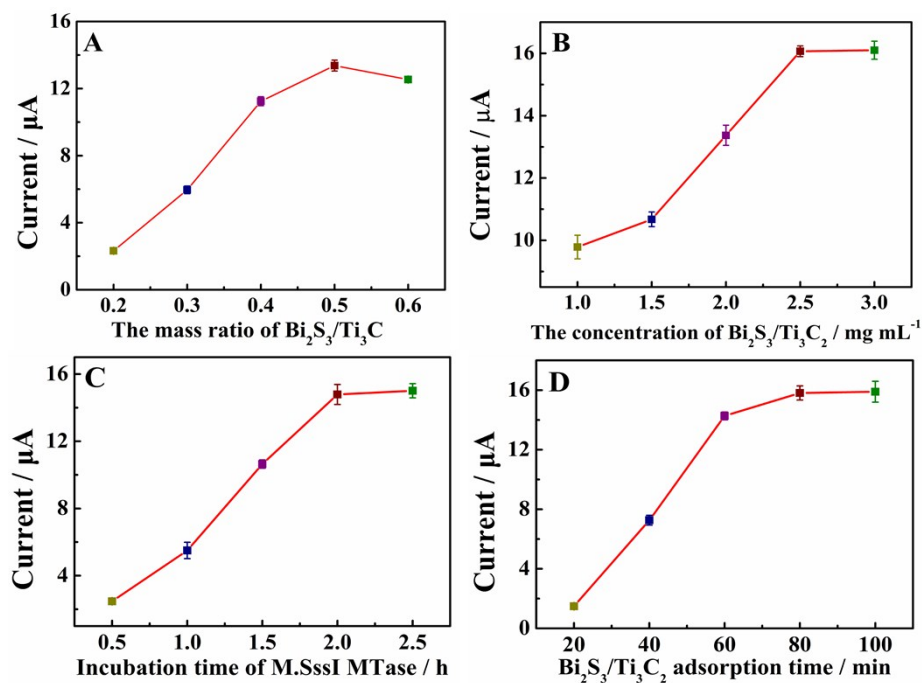


Fig. S10 Influences of some parameters on photocurrents of the PEC biosensing platform.

(A) The mass ratio of Bi₂S₃/Ti₃C₂ (Bi₂S₃/Ti₃C₂ concentration, 2.0 mg mL⁻¹; M.SssI MTase incubation time, 2 h; Bi₂S₃/Ti₃C₂ adsorption time, 80 min); (B) The concentration of Bi₂S₃/Ti₃C₂ (Bi₂S₃/Ti₃C₂ mass ratio, 0.5; M.SssI MTase incubation time, 2 h; Bi₂S₃/Ti₃C₂ adsorption time, 80 min); (C) The incubation time of M.SssI MTase (Bi₂S₃/Ti₃C₂ mass ratio, 0.5; Bi₂S₃/Ti₃C₂ concentration, 2.5 mg mL⁻¹; Bi₂S₃/Ti₃C₂ adsorption time, 80 min); (D) The adsorption time of Bi₂S₃/Ti₃C₂ nanosheets (Bi₂S₃/Ti₃C₂ mass ratio, 0.5; Bi₂S₃/Ti₃C₂ concentration, 2.5 mg mL⁻¹; M.SssI MTase incubation time, 2 h).

16. Comparison of various PEC biosensors for M.SssI MTase activity assay

Table S1. Comparison of various PEC biosensors for M.SssI MTase activity assay.

Materials	Linear range (U mL⁻¹)	Detection limit (U mL⁻¹)	Signal-to- noise ratio*	Reference
Bi ₂ S ₃	1-50	0.33	1.3	[5]
TiO ₂ /CdTe QDs & GQDs@ZIF-8	0.005-150	0.004	0.3	[6]
SnO ₂ & Ru(bpy) ₂ (dppz) ²⁺	5-80	0.45	1.6	[7]
g-C ₃ N ₄ & CdS QDs	1-80	0.316	3.4	[8]
BiOI	0.1-50	0.035	0.7	[9]
TiO ₂ & CdSe QDs	0.01-150	0.0042	0.5	[10]
Bi ₂ S ₃ /Ti ₃ C ₂	0.01-30	0.003	136.4	This work

*Signal-to-noise ratio = I/I_0 , where I is the photocurrent of the biosensor incubated with 30 U mL⁻¹ M.SssI MTase, I_0 is the photocurrent without M.SssI MTase.

17. Selectivity, stability, reproducibility and recovery test

Taking AIuI MTase and Dam MTase as interferents, the selectivity of this biosensing platform was investigated. As shown in Fig. S11A, no obvious response photocurrent can

be observed for AflI MTase (150 U mL^{-1}) and Dam MTase (150 U mL^{-1}), compared with that for M.SssI MTase (15 U mL^{-1}), indicating a good selectivity of the proposed biosensing platform. Moreover, the stability is further investigated after storing the developed biosensor at $4 \text{ }^{\circ}\text{C}$ for two weeks. It is noted that the response photocurrent still remains 93.9 % of the initial value for 15 U mL^{-1} M.SssI MTase, implying an acceptable stability of the biosensing platform. In addition, the reproducibility of the prepared biosensing platform is also investigated. The relative standard deviation (RSD) for five electrodes is 2.8 %, suggesting a good reproducibility.

To explore the practical application of the proposed biosensor in M.SssI MTase activity assay, normal human serum samples were used to simulate the complex environment. The 10-fold diluted human serum solutions (diluted with $1 \times \text{NEBuffer 2}$) were spiked with different concentrations of M.SssI MTase (1, 10 and 20 U mL^{-1}). As shown in Fig. S11B, the response photocurrents in these human serum samples are almost the same as that in $1 \times \text{NEBuffer 2}$. In addition, the recoveries in human serum samples for the added M.SssI MTase with 1, 10 and 20 U mL^{-1} are 98.0 %, 104.0 % and 92.7 %, respectively (Table S2), confirming that the proposed PEC biosensing platform possesses promising applications in M.SssI MTase activity assay in real samples.

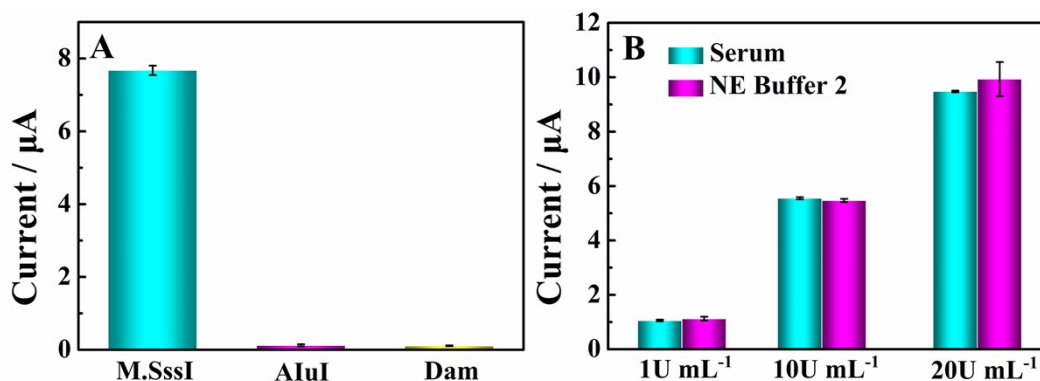


Fig. S11 (A) Selectivity of the PEC biosensing platform toward M.SssI MTase. (M.SssI MTase, 15 U mL⁻¹; interfering substances, 150 U mL⁻¹). (B) Comparison of the M.SssI MTase activity assay in human serum and NE Buffer 2.

Table S2. Recovery assay for M.SssI MTase in the human serum samples.

Sample	Added (U mL ⁻¹)	Found (U mL ⁻¹)	RSD (%)	Recovery (%)
1	1.0	0.98	3.1 %	98.0 %
2	10.0	10.4	4.0 %	104.0 %
3	20.0	18.5	3.2 %	92.7 %

*Average value of three measurements.

18. Efficiency of different inhibitors on M.SssI MTase activity

Abnormal DNA methylation is always associated with various kinds of diseases or cancers.^[11,12] Screening the effective inhibitors for DNA methylation is a significant research. Up to now, there are mainly two categories of inhibitors for DNA methylation. One of them is nucleoside analogs, and the other is non-nucleoside analogs. In order to

verify the proposed analytical method is able to screen the DNA methylation inhibitors, one of the nucleoside analogs and one of the non-nucleoside analogs are selected as the model (Fig. S12). And the inhibition efficiency (%) is estimated as follows: Inhibition (%) = $(I_1 - I_2) / (I_2 - I_0) \times 100\%$. Where I_0 , I_1 , and I_2 represent the photocurrent in the absence of M.SssI MTase, in the presence of M.SssI MTase, and in the presence of both M.SssI MTase and inhibitor, respectively.^[13] Taking the half maximal inhibitory concentration ($I_{c_{50}}$) represent the inhibiting efficiency, the $I_{c_{50}}$ value can be calculated to be 1.9 μM for 5-Aza-2'-dC (Fig. S12A), which are consistent with the reported literatures.^[14,15] In addition, the $I_{c_{50}}$ value for procaine is 21.2 μM (Fig. S12B). These results indicate that the proposed PEC method has a potential application in screening of the DNA methylation inhibitor.

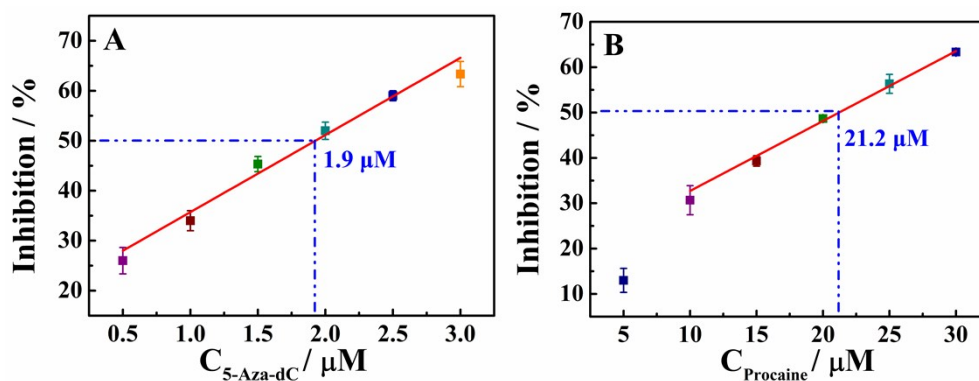


Fig. S12 The inhibition effect of 5-Aza-2'-dC (A) and Procaine (B) for the activity of M. SssI MTase (30 U mL^{-1}).

19. Reference

- [1] S. Wang, S. Wei, S. Wang, S X. Zhu, C. Lei, Y. Huang, Z. Nie and S. Yao, *Anal. Chem.*, 2019, **91**, 1651-1658.
- [2] Y. Fu, K. Zou, M. Liu, X. Zhang, C. Du and J. Chen, *Anal. Chem.*, 2019, **92**, 1189-1196.
- [3] X. Peng, Y. Zhang, D. Lu, Y. Guo and S. Guo, *Sens. Actuators, B*, 2019, **286**, 222-229.
- [4] H. Wang, R. Zhao, J. Qin, H. Hu, X. Fan, X. Cao and D. Wang, *ACS Appl. Mater. Interfaces*, 2019, **11**, 44249-44262.
- [5] Z. Yang, F. Wang, M. Wang, H. Yin and S. Ai, *Biosens. Bioelectron.*, 2015, **66**, 109-114.
- [6] L. Meng, K. Xiao, X. Zhang, C. Du and J. Chen, *Biosens. Bioelectron.*, 2019, 111861.
- [7] X. Liu, C. Wei, J. Luo, Y. Wu, X. Guo, Y. Ying, Y. Wen and H. Yang, *Microchim. Acta*, 2018, **185**, 498.
- [8] H. Wang, P. Liu, W. Jiang, X. Li, H. Yin and S. Ai, *Sens. Actuators, B*, 2017, **244**, 458-465.
- [9] Y. Zhou, Z. Xu, M. Wang, B. Sun, H. Yin and S. Ai, *Biosens. Bioelectron.* 2014, **53**, 263-267.
- [10] Q. Shen, L. Han, G. Fan, E. S. Abdel-Halim, L. Jiang and J. J. Zhu, *Biosens. Bioelectron.*, 2015, **64**, 449-455.
- [11] S. Mastoraki, A. Strati, E. Tzanikou, M. Chimonidou, E. Politaki, A. Voutsina, A. Psyrris, V. Georgoulas and E. Lianidou, *Clin. Cancer Res.*, 2018, **24**, 1500-1510.

- [12] A. Koch, S. C. Joosten, Z. Feng, T. C. de Ruijter, M. X. Draht, V. Melotte, K. M. Smits, J. Veeck, J. G. Herman, L. Van Neste, W. Van Crieckinge, T. De Meyer and M. van Engeland, *Nat. Rev. Clin. Oncol.*, 2018, **15**, 459-466.
- [13] M. Wang, Z. Xu, L. Chen, H. Yin and S. Ai, *Anal. Chem.*, 2012, **84**, 9072-9078.
- [14] Q. Hong, L. Ge, W. Wang, X. Liu and F. Li, *Biosens. Bioelectron.*, 2018, **121**, 90-95.
- [15] L. Meng, K. Xiao, Y. Li, X. Zhang, C. Du and J. Chen, *Chem. Commun.*, 2019, **55**, 8166-8169.